

1 **Report 2**

2 **Reply to Anonymous Referee #1**

3 This article develops a numerical method for simultaneously retrieving AOD, SSA and
4 DHR from DPC multi-angle polarimetry (MAP) observations. The authors analyze the
5 sensitivities of both scalar and polarimetric reflectance to SSA, and get reliable results of
6 global AOD, SSA, and DHR based on the retrieval algorithm. As one of the few operational
7 spaceborne MAP sensors, inversion algorithms based on DPC observations, particularly
8 those for SSA retrieval, remain quite limited, with few global SSA products currently
9 available. This study provides a reference for the design of future MAP sensors and the
10 development of aerosol retrieval algorithms. The global SSA maps presented in this article
11 also provide valuable insights into aerosol scattering and absorption characteristics in
12 recent years. However, several aspects of the data, methods, and results require further
13 clarification and improvement.

14 We thank the reviewer for the detailed comments and thoughtful suggestions, which are
15 very helpful in improving our manuscript. We have carefully addressed all concerns and
16 revised the manuscript accordingly. A point-by-point response is presented below.

17 **General comments:**

18 1. Data used in the article: The authors retrieve aerosol and surface parameters from
19 DPC measurements, and validate the retrieved results according to comparing with
20 AERONET and MODIS products. However, there are several points need to be
21 clarified. (1) DPC data: The description of DPC data is not very clear. The authors
22 introduce that DPC provide observations across 8 spectral bands, but only 5 bands
23 are mentioned in Section 2.1. Moreover, the use of polarized observations is also
24 not specified. (2) AERONET data: The authors use all the Level 2.0 quality control
25 criteria except AOD threshold to screen the AERONET Level 1.5 SSA. But the 0.4
26 AOD threshold are still utilized to screen the SSA in the validation progress. Why

27 not directly utilize the Level 2.0 SSA data? (3) The periods of DPC and AERONET
28 data used in the article are not specified.

29 We thank the reviewer for the suggestion about the usage of data in the article.

30 (1) DPC data: We have revised the manuscript and listed all the DPC channels in L73:
31 *The sensor provides measurements across 8 spectral bands (443, 490, 565, 670,*
32 *763, 765, 865, and 910 nm) from visible to near-infrared wavelengths.*

33 The use of DPC observations have been listed in Table 2 and clarified in L167:

34 *The measurement vector, \mathbf{y} , is constructed with calibrated scalar reflectance at 443,*
35 *490, 565, and 670, as well as DOLP at 490 and 670 nm from several angles.*

36 (2) AERONET data.

37 Although AERONET Level 2.0 SSA data provide the highest quality, the number of
38 available Level 2.0 SSA retrievals during the study period (6 months) is very limited, which
39 would not allow a statistically meaningful validation of the algorithm performance. In order
40 to balance the data quality and data availability, all Level 2.0 quality control criteria except
41 for the AOD threshold were applied to the Level 1.5 data. Moreover, the AOD threshold
42 ($\text{AOD}_{440} > 0.4$) was applied only in the SSA validation step and was based on the
43 retrieved AOD, rather than the AERONET AOD. This filtering was introduced to exclude
44 cases with insufficient sensitivity of the measurements to SSA, and it was not applied to
45 the validation of AOD or DHR. Therefore, quality-controlled AERONET Level 1.5 data
46 were used in this study.

47 (3) Periods of data:

48 We thank the reviewer for pointing out this missing information. In the revised manuscript,
49 we have explicitly specified the time periods of both the DPC and AERONET data used in
50 this study. Six months of DPC Level 1 data, covering April, July, and October 2019, as
51 well as January–March 2020, are used for the retrieval. The AERONET observations used
52 for validation correspond to the same periods as the DPC overpasses. This information has
53 been added in L75:

54 *Six months of DPC Level 1 data, encompassing April, July, and October 2019, as*
55 *well as January-March 2020, are used in the retrieval in this study. The AERONET,*
56 *MODIS, as well as other auxiliary data are selected from the same periods.*

57 2. Retrieval algorithm: The authors have provided a detailed description of the
58 retrieval algorithm, but the introduction to the flowchart could be strengthened by
59 providing more details. The authors can consider the following aspects. (1) The
60 DPC observations have “up to 12 viewing angles” and typically “exceeding 9
61 angles”. Are observations from all the angles used for inversion? What about those
62 pixels with viewing angles less than 9? (2) Which method is employed to minimize
63 the cost function? (3) What criteria are utilized for the matching of DPC and
64 AERONET data?

65 We thank the reviewer for the suggestion about the retrieval algorithm in the article.

66 (1) In this study, only pixels with at least 9 valid viewing angles were used for the
67 inversion. Pixels with fewer than 9 viewing angles, which are primarily located
68 near the scan edges, were excluded to ensure sufficient angular sampling. For the
69 remaining pixels, observations from the first 9 viewing angles were used for the
70 retrieval to maintain a consistent angular configuration across all pixels. We have
71 added the relevant description in the manuscript in L170:

72 *However, most pixels are observed from more than 9 viewing angles. Pixels with*
73 *fewer than 9 viewing angles, which are primarily located near the scan edges, were*
74 *therefore excluded. For the remaining pixels, observations from the first 9 viewing*
75 *angles were used in the retrieval to maintain a fixed number of viewing angles for*
76 *all pixels. Consequently, the scalar reflectance and DOLP at each wavelength*
77 *consist of measurements acquired from 9 viewing angles.*

78 (2) In this study, the cost function is minimized using an iterative Gauss–Newton
79 method. This information has been added to the revised manuscript in L201:

80 *The algorithm minimizes the cost function defined in Eq. 4 using an iterative*
81 *Gauss–Newton method to obtain the final retrieval results.*

82 (3) In the numerical simulation experiments, daily AERONET data are used to describe
83 representative aerosol parameters, and a spatial collocation radius of 8 km is used.
84 We have added the relevant description in the manuscript in L223:

85 *The simulated dataset was constructed using aerosol parameters derived from daily*
86 *AERONET observations selected within an 8 km radius of DPC overpass locations*
87 *to represent typical aerosol conditions observed by DPC. The corresponding*
88 *viewing geometry, including SZA, VZA, and RAA, was taken from the matched DPC*
89 *observations and used in the radiative simulations, thereby accounting for the*
90 *actual scattering angle distribution of DPC observations.*

91 3. Validation results: The authors analyzed several statistical indicators (e.g.,
92 correlation coefficient, RMSE, bias) to validate retrieval results. For SSA
93 validation, the ratio of points falling within the Error Envelope (EE) is also a useful
94 indicator to assess the result. It would be helpful to add EE lines to the figures and
95 annotate the corresponding point ratios.

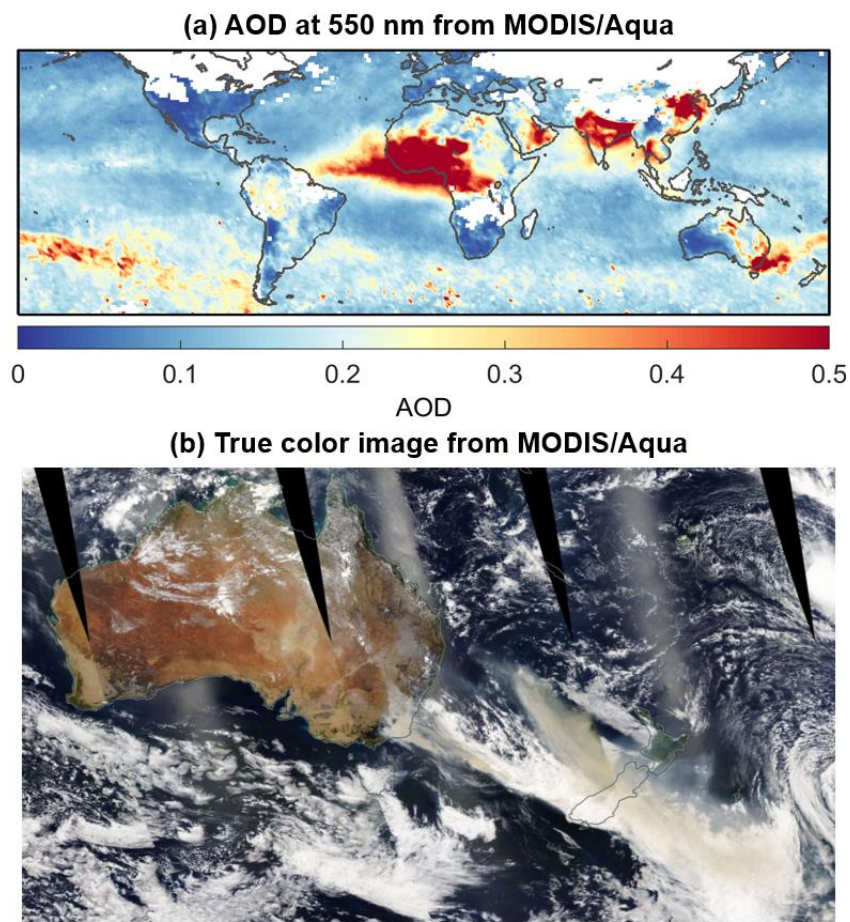
96 Thanks for the very helpful suggestion. We have added the ± 0.03 Error Envelope (EE)
97 lines to the SSA validation scatter plot and indicated the proportion of samples falling
98 within the EE in the figure. Corresponding analysis has also been added in the manuscript.

99 4. Global maps: Section 5 shows global retrieval results. These maps provide valuable
100 insights into aerosol and surface properties. I have two comments about these
101 results. (1) The authors explain that the zonal discontinuities in the maps are
102 primarily due to defects in the original data. However, the discontinuities observed
103 over oceanic areas also seem to be related to the incompletely filtered clouds.
104 Would be better to clarify in the manuscript. (2) Heavy AOD is observed over
105 Southern Oceans in January 2020. The authors attribute it to the strong Australian
106 wild fires. However, the AOD over Southern Oceans almost reaches 0.5 in Fig.
107 10(d). Is this magnitude reasonable? Was it also observed by other sensors?

108 We thank the reviewer for the helpful comments.

109 (1) We agree that the zonal discontinuities observed over oceanic regions may also be
110 related to incompletely filtered clouds, in addition to defects in the original data. In

111 this study, cloud screening also relies on observations at 865 nm, which have not
112 been re-calibrated and can have higher uncertainties (up to about 23%). As a result,
113 cloud pixels may not be completely removed. We have revised the manuscript to
114 clarify this limitation and added a discussion acknowledging that residual cloud
115 effects related to the cloud screening procedure may contribute to the observed
116 discontinuities.



117

118 **Fig. R2-1. (a) Global AOD for January 2020 at 550 nm from MODIS/Aqua Level 3 product. (b)**
119 **True color image from MODIS/Aqua on January 1, 2020.**

120 (2) As for the abnormally high AOD values observed over the Southern Ocean, we
121 conducted further examinations using true-color imagery and MODIS AOD
122 products. The true-color imagery (Fig. R2-1b) for early January 2020 reveals
123 extensive smoke plumes over the Southern Ocean originating from southeastern
124 Australia and gradually transported eastward. This indicates that large amounts of

125 biomass-burning aerosols were present over the region during this period. The
126 MODIS monthly AOD product for January 2020 also shows anomalously high
127 AOD over the Southern Ocean, with values exceeding 0.5 in some areas (Fig. R2-
128 1a). The spatial pattern and magnitude are generally consistent with our retrieval
129 results. Thus this magnitude is likely reasonable. We have added the corresponding
130 MODIS AOD map to the Supplement material, and included a relevant discussion
131 in the manuscript in L440:

132 *The anomalously high AOD over the Southern Ocean in January 2020 reaches*
133 *values of up to 0.5 in some regions, consistent with independent data sources (e.g.,*
134 *MODIS AOD, see Supplement).*

135 **Minor comments:**

136 1. L68: The calculation of DOLP is not described in the article.

137 Thanks for reminding. We have added an equation (Eq. 7) of calculating DOLP in the
138 manuscript in Sect. 2.6.

139 2. Fig. 2-4: Please explain the x label “scat_ang” in the caption.

140 Thanks for reminding. The xlabel “scat_ang” refers to “scattering angle”, and we have
141 explained in the caption of Fig. 2.

142 3. Fig. 7: DHR data are not AERONET observations. Please revise the caption.

143 Thanks for reminding. We have revised the caption of Fig. 7 to clarify the data sources:

144 *Comparison between retrieved AOD (left) and SSA (middle) at 443 nm and*
145 *AERONET observations, and comparison between retrieved DHR (right) at 443 nm*
146 *and the MODIS product.*

147 4. Section 3.2: Please keep the number of significant digits consistent.

148 Thanks for pointing it out. We have carefully checked Section 3.2 and revised the
149 manuscript to ensure that the number of significant digits is used consistently throughout
150 this section.

151 5. Fig. 8: The “(a)/(b)/(c)” labels are not marked in the figures.

152 Thanks for reminding. We have added labels in Figs. 8 and 9.

153 6. Figs. 8-12: The wavelength labeled in the figures (440 nm) does not match the
154 wavelength mentioned in the text (443 nm). Please update either the figures or the
155 relevant text for consistency.

156 Thanks for pointing out this inconsistency. The wavelength labels have been carefully
157 checked and updated for consistency. All references have now been unified to 443 nm in
158 both the figures and the corresponding text.